International Journal of
STEEL STRUCTURES

Seismic Response of Base Isolating Systems with U-shaped Hysteretic Dampers

Sang-Hoon Oh[1], Sung-Hoon Song[2], Sang-Ho Lee[3], and Hyung-Joon Kim[4]*

[1]*Associated Professor, Department of Architectural Engineering, Pusan National University, Korea*
[2]*Ph.D. Student, Department of Architectural Engineering, Pusan National University, Korea*
[3]*Professor, Department of Architectural Engineering, Pusan National University, Korea*
[4]*Assistant Professor, Department of Architectural Engineering, University of Seoul, Korea*

Abstract

This paper proposes a base isolating system to reduce the seismic demands of low- or medium-rise structures and experimentally investigates its seismic response using shake-table tests. The base isolating system considered in this study consists of laminated-rubber bearings and U-shaped hysteretic (UH) dampers which are made of high toughness steel (HTS) and are machined with slotted holes to increase their deformation capacities. A base isolated 2-story specimen for shake-table tests was first designed and cyclic tests of laminated-rubber bearings and UH dampers implemented in the base isolating systems were then carried out. The component test for the laminated-rubber bearings shows typically low lateral stiffness with enough vertical stiffness to carry gravity loads. The test results for the UH dampers demonstrate that the use of HTS material and the introduction of the slotted holes details increase deformation capacities by inducing uniform stress distribution along a UH damper. Finally, shake-table tests were performed using specimens shaken with increasing ground acceleration records. The shake-table tests show that the proposed base isolating system with UH dampers limits the seismic demands of a base isolated structure by lengthening its structural period, concentrating displacement demands on the base isolating floor and adding seismic energy dissipation from the UH dampers.

Keywords: U-shaped hysteretic damper, deformation capacity, base isolation, slotted holes, shake-table tests

1. Introduction

Current seismic design philosophy intends that ordinary structures remain within an elastic range or experience minor structural damages under frequent earthquakes with a probability of exceedence of 50% in 50 years while allowing them to suffer major structural damages under a design-based earthquake with a probability of exceedence of 10% in 50 years (SEAOC, 1995; BSSC, 1997; ASCE, 2000; BSSC, 2003). However, this is contrary to the public's expectation that structures engineered according to current seismic codes be in function immediately after a design-based earthquake. Socio-economic developments have significantly raised the required performance level of structures and seismic risk defined as loss of life and economic loss in urban areas has also increased because of the dense urbanization that has taken place worldwide.

During the last thirty years, the use of base-isolation technologies has been widely used to meet the building owner's desire and to achieve higher seismic performance of structures. Their basic concepts had fist been used for bridge construction to accommodate temperature-induced movements and deformations. Building structures started then to employ these technologies. By decoupling a structure from ground shaking, seismic isolation significantly reduces its structural damage which is potentially expected in conventional, fixed-base buildings (Kelly, 1979; 1990). The decoupling is achieved by the bearings with low lateral stiffness while they must provide the high stiffness in the vertical direction to rigidly support gravity loads of a building. Laminated-rubber bearings composed of elastomeric rubber layers alternating with steel plates are commonly used for the seismic isolation because the vertical stiffness of rubber layers with the low lateral stiffness is significantly enhanced by the presence of the steel plates vulcanized to the rubber layers (Christopoulos and Filiatrault, 2006). Also, the bulging deformation of the rubber is delayed by the confinement of the steel

*Corresponding author
 Tel: +82-2-2210-5794; Fax: +82-2-2248-0382
 E-mail: hyungjoonkim@uos.ac.kr

Ⓐ Springer
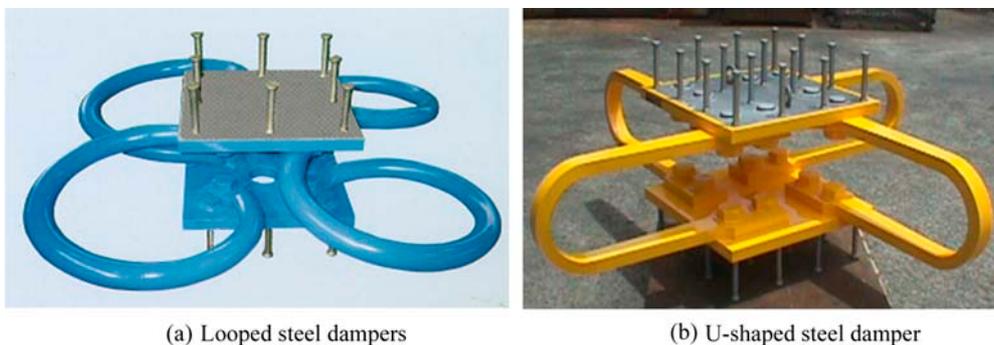
(a) Looped steel dampers   (b) U-shaped steel damper

Figure 1. Steel hysteretic dampers for seismic isolation systems.

plates so that the stability of bearings under lateral loading is improved.

However, large lateral deformation demands resulting stability problems occur at the seismic isolation system due to the low damping and lateral stiffness of laminated-rubber bearings. In order to address this, high damping rubbers have been more recently suggested for laminated-rubber bearings (Hwang and Ku, 1997; Pan *et al*., 2004). Although base isolators using high damping rubbers have displayed significant increased energy dissipating capabilities, high damping rubber has still material inherent problems that it is susceptible to heat-related property changes during cyclic loading and to aging effects influencing stiffness and energy dissipation capacity (Pan *et al*., 2004). Another way to increase energy dissipation of laminated-rubber bearings is to add external components such as lead plugs inserted in the center of the bearing (Robinson, 1982; Skinner *et al*., 1993). But the use of lead plugs as energy dissipating devices is hesitated because of health and environmental concerns.

For this reason, supplemental energy dissipating devices such as hysteretic or viscous dampers have been suggested as an alternative to lead plugs (Tyler, 1977; Teramura *et al*., 1988; Cousins *et al*., 1991; Parducci and Mezzi, 1991; Skinner *et al*., 1993). Steel hysteretic dampers, as shown in Fig. 1, could be one of candidates for seismic energy dissipating devices applicable to base isolation systems. The limited deformation and energy dissipating capacity of steel, compared to lead plugs, have to be overcome for the applications to base isolation systems where large deformation demands are concentrated. Recently, steel dampers shown in Fig. 1 (b) were developed as energy dissipating devices for a base isolation system and consisted of several U-shaped steel strips made from rolled steel, SN490B specially designed for enhancing their deformation capacities. Suzuki *et al*. (2005) carried out cyclic tests of U-shaped hysteretic (UH) dampers under different strain velocities and temperature. Test results showed that the UH dampers developed stable hysteretic cyclic response even at significantly large imposed displacement in both horizontal directions.

In this paper, UH dampers made from high toughness

steel (HTS) of which the chemical composition is different with that of ordinary structural steel are proposed as supplemental energy dissipating devices applicable to base isolation systems. Furthermore a new detail for UH dampers is developed for inducing uniform stress distribution on the steel strip and for consequently increasing their deformation capacities. The proposed detail consists of a series of slotted holes distributed along a U-shaped steel strip to prevent premature failures due to stress concentration that would occur at UH dampers without the proposed detail.

In order to investigate the seismic response of seismic isolated structures with UH dampers manufactured with slotted holes, a two-story frame specimen with base isolating systems was first designed according to an energy based design method and main components of a base isolating system, laminated-rubber bearings and UH dampers, were also sized. Experimental validation for the main components was carried out to evaluate their structural characteristics and to confirm the displacement capacities and cyclic response of a UH damper with the proposed detail. Two frame specimens were prepared for the shake-table tests. One of them was manufactured as a fix-based frame structure while the UH damped base isolating system was implemented into the other. Results obtained from the shake-table tests of two specimens were used to compare the seismic response of the fix-based and the base isolated structures.

2. Design of Shake-Table Specimen with U-Shaped Hysteretic Damped Base Isolation Systems

2.1. Energy based seismic design for base isolated structures

Energy based seismic design methodology has been commonly used for the design of base isolated structures. The theoretical background on the energy based seismic design methodology describing in this paper is referred to Soong and Dargush (1997). In the energy balance design method, a structure shall be designed to satisfy Eq. (1):

$$E_T \geq E_G \tag{1}$$

where E_T is the total energy that the structure can dissipate (and/or absorb) and E_G is the seismic input energy into the structure during ground shaking. The total energy E_T of a single-degree-of-freedom system consists of the kinetic energy E_k, the dissipated energy E_h by inherent damping mechanism, and the total amount of energy E_a that the structure has absorbed through elastic straining or unrecoverable inelastic deformations of its elements.

$$E_T = E_k + E_h + E_a = \int_0^{t_0} m\ddot{x}\dot{x}\,dt + \int_0^{t_0} c\dot{x}^2\,dt + \int_0^{t_0} F(x,\dot{x})\dot{x}\,dt \tag{2}$$

where t_0 is the duration of ground shaking; m, c, and F are the mass, the equivalent viscous damping constant and the restoring force of the system, respectively; x, $\dot{x}$, $\ddot{x}$ and are the relative displacement, velocity, and acceleration, respectively. The kinetic energy E_k and the dissipated energy E_h in a base isolating system can be calculated by:

$$E_k = \int_0^{t_0} m\ddot{x}\dot{x}\,dt = \frac{Q_{m,f}\delta_m}{2} \tag{3}$$

$$E_h = \int_0^{t_0} c\dot{x}^2\,dt = 4\pi k_f\,\xi_f\,d_m^2 \tag{4}$$

where $Q_{m,f}$, δ_m, and k_f are the maximum lateral force, corresponding displacement and stiffness of laminated-rubber bearings, respectively; ξ_f is the damping ratio added by, if any, laminated-rubber bearing. Since the energy absorbed through elastic straining is almost zero at the end of ground shaking, E_a equals to the energy due to unrecoverable inelastic deformations of its elements and is estimated by:

$$E_a = \int_0^{t_0} F(x,\dot{x})\dot{x}\,dt = \eta Q_{Y,s}\delta_m \tag{5}$$
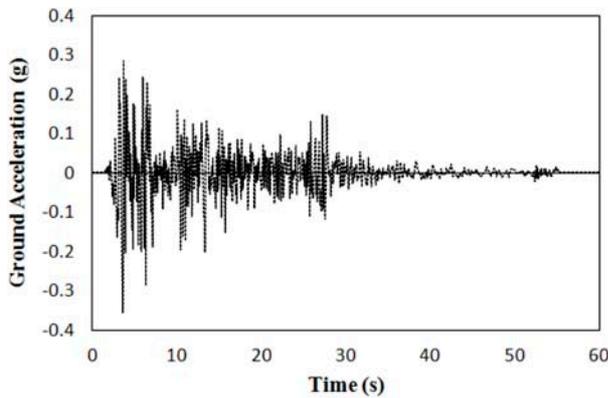
where $Q_{Y,s}$ is the yield strength of energy dissipating devices in base isolating systems and η is a constant which determines the relation between E_a and the energy dissipated during a half cycle at the maximum displacement of a base isolating system. Akiyama (1985; 1988) found from nonlinear time-history analysis that the accumulated plastic deformation of an elasto-perfect plastic single-degree-of-freedom system during ground shaking is approximately equal to 8 times the maximum deformation δ_m. The add of energy dissipating devices into base isolating systems increases the base shear of a base isolated structure even if the displacement across the isolating plane is decreased. It is noted that the increase in E_a by energy dissipating devices does not always provide beneficial effects on the design of base isolated structures.

The seismic energy E_G input into a structure subjected to ground acceleration is calculated from:

$$E_G = \int_0^{t_0} m\ddot{x}_g\dot{x}\,dt \tag{6}$$

Housner (1956; 1959) demonstrated that E_G is very stable value depending on the fundamental period of a structure rather while it is negligibly affected by the distribution of mass, stiffness and strength. In the energy balance design method, energy equivalent velocity spectrum V_E is usually used instead of E_G. The relation between E_G and V_E is expressed by:

$$E_G = \frac{V_E^2}{2} \tag{7}$$

Figure 2 shows the energy equivalent velocity spectrum of elastic structures subjected to ground acceleration obtained from the Elcentro earthquake with the peak ground acceleration of 0.364 g. For design purposes and conservative approach, the energy equivalent velocity spectrum is assumed as V_{EM} which is generally simplified

(a) Ground acceleration obtained from Elcentro earthquake
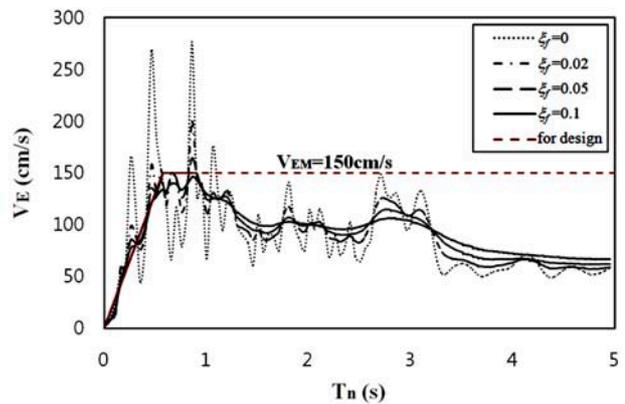
(b) Energy equivalent velocity spectrum with different damping ratios

Figure 2. Energy equivalent velocity spectrum.

to bilinear curves, as a dotted line shown in Fig. 2.

For the design of a base isolating system, substituting Eq. (3), (4), (5) and (7) into Eq. (1) gives

$$\frac{Q_{m,f}\delta_m}{2}+8Q_{Y,s}\delta_m \geq \frac{mV_{EM}^2}{2} \tag{8}$$

with the assumption that the supplemental damping ratio ξ_f by laminated-rubber bearings is zero.

2.2. Design of an isolated structure for shake-table tests

In order to investigate seismic response of a structure with base isolating systems equipped with UH dampers, a steel moment-resisting frame (MRF) was designed as an isolated structure. The target period of a MRF was set to 0.5 to 0.6 second representing the fundamental periods of low-, and medium-rise steel structures. Considering the circumstance of a structural laboratory to be performed shake-table tests, a two-story steel MRF with 2.5 meter story height was, as shown in Fig. 3, chosen as an isolated structure. The footprint size of the isolated structure was decided to 3.5 meter by 2.5 meter based on the size of the shake-table. The isolated structure was assumed to be excited in the direction of the column weak axis which is the same as the long direction of the isolated structure. Seismic mass of 15 metric ton was assumed to be mounted on each floor.

In order to size its columns and beams, the isolated structure was assumed as a shear building which horizontal members have infinite stiffness for preliminary design. Based on the geometric condition and mass distribution, W-shape rolled steel columns and beams for the isolated structure were sized by iterative calculation works. Table 1 summarizes the structural properties of the selected columns and beams in the isolated MRF test specimen. After selecting column and beam members, eigenvalue analysis was performed with consideration of beam flexibilities using commercial structural analysis software, MIDAS Gen (2008). Analysis results show that the 1st and 2nd vibration periods are, respectively, 0.54 and 0.204 second.

2.3. Design of base isolating isolators

Based on the fundamental period, 0.54 second of an isolated structure and the energy equivalent velocity for the design, V_{EM}=150 cm/sec, as shown in Fig. 2(b), the target period T_f by base isolators was set to 3.0 second. For shake-table tests, two laminated-rubber bearings were assumed to be installed and each laminated-rubber bearing consequently supports vertical loads Wo of 150 kN. The shear modulus Gf of a laminated-rubber bearing obtained from the specification provided by manufacturers is 0.30 MPa.

The required lateral stiffness $K_{f,req}$=67 N/mm of the laminated-rubber bearing is obtained from:

$$K_{f,req}=\frac{4\pi^2}{T_f^2}\frac{W_o}{g} \tag{9}$$

(a) Framing plan　　　　(b) Elevation
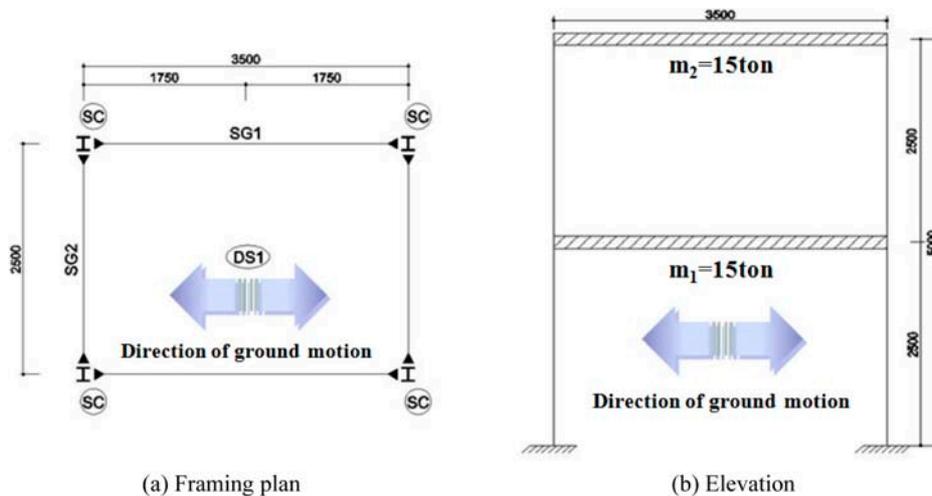
Figure 3. Dimensions of an isolated structure.

Table 1. Structural properties of members in steel MRF test specimen

Member	Dimensions (mm)				Section area (mm²)	Unit weight (N/m)	Moment of inertia (x10⁴mm⁴)	
	overall height	flange width	web thk.	flange thk.			I_x	I_y
Columns	350	175	7	11	6,314	496	13,600	984
Beams	300	150	6.5	9	4,678	367	7,210	508

Table 2. Dimension of a base isolator (laminated-rubber bearing)

Rubber sheets		Steel plates				
Thickness t_R (mm)	Number of layers, n_R	Thickness of inner plate $t_{S,in}$ (mm)	Thickness of end plate $t_{S,in}$ (mm)	Outer diameter D_O (mm)	Inner diameter D_I (mm)	Section area A_f (mm^2)
4.2	25	2.3	22	200	100	23,560

with the values of G_f=0.30 MPa and $K_{f,req}$=67 N/mm, a laminated-rubber bearing is sized the following equation:

$$K_{f,req} = \frac{G_f \, \gamma_f \, A_f}{n_R t_R \gamma_f} = \frac{G_f \, A_f}{n_R t_R} \qquad (10)$$

where A_f, n_R, and t_R are the effective area of the laminated-rubber bearing and the number and thickness of rubber layers in the laminated-rubber bearing and γ_f is the shear strain of a base isolator. The dimensions A_f, n_R, and t_R of a laminated-rubber bearing were chosen to satisfy $K_{f,req}$=67 N/mm and are presented in Table 2.

2.4. Design of energy dissipating devices

Energy dissipating devices are usually implemented in a base isolated structure in order to reduce the seismic demand at a base isolation floor. In this experimental study on the seismic response of base isolated structures, UH dampers shown in Fig. 4 (a) are used as energy dissipating devices. Equation (8) gives the maximum lateral force $Q_{m,f}$ resisted by a laminated-rubber bearing is 12.4 kN and the yield strength $Q_{Y,s}$ of UH dampers attached at a laminated-rubber bearing is 10.8 kN throughout iterative calculations using V_{EM}=1,50 cm/sec, $K_{f,req}$=67 N/mm, the weight of 150 kN mounted on a single base isolator and the shake table capacity. Note that the maximum deformation δ_m=185 mm is computed according to the equation proposed by Akiyama (1985; 1988):

$$\delta_m = \frac{T_f \, V_{EM}}{2\pi} \frac{1}{\sqrt{2\eta - 1}} \qquad (11)$$

Therefore, the base shear of a base isolated frame is
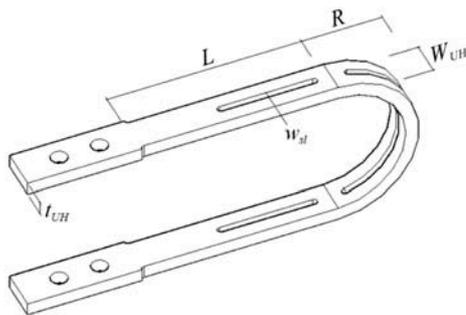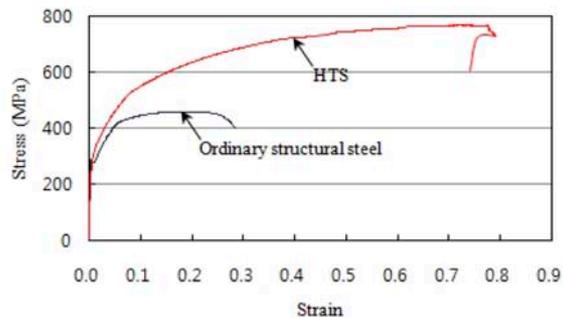
46.4 kN which is two times the sum of $Q_{m,f}$ and $Q_{Y,s}$. It is noted that the seismic coefficient of about 15.5% (=base shear/seismic weight) used for the design of test specimens is high for practical applications of base isolated structures. For practical applications, the sophistic evaluation is required for the values of V_{EM} and η that are conservatively estimated in the preliminary design phase.

Significantly large deformation capacity is required for UH dampers since displacement demand of a base isolated structure is concentrated on the isolated floor. UH dampers are made from High toughness steel (HTS) of which the chemical composition is different with that of ordinary structural steel and the manganese content is considerably increased. Large portion of manganese in steel composition leads the desirable mechanical properties, increased deformation capacities and large ratio of ultimate strength to yield strength, in seismic applications. Figure 4 (b) shows the stress-strain curve of HTS and also present that of ordinary structural steel for comparison. Three coupon tests were carried out to find out the mechanical properties of HTS and the elastic modulus E_S=190 GPa, the yield strength F_Y=264 MPa, and the ultimate strength F_U=775 MPa were examined in an average basis.

In addition to the increase of deformation capacity using HTS, slotted holes on a UH damper are introduced to induce uniform stress distribution at significantly large deformation levels, which results in the increase of its deformation capabilities. The slotted holes are located in the middle of width of a steel strip. Kwon (2008) proposed the introduction of slotted holes on a UH damper in order to increase its deformation capacity and confirmed the effect of slotted holes throughout experiments and analyses with the study parameters, types of steel material,

(a) UH damper with slotted holes

(b) Stress-strain curves of HTS of ordinary structural steel for comparison

Figure 4. Mechanical properties and Shape of UH dampers.

Table 3. Dimensions of a UH damper

Radius R, mm	Length of flatted part L, mm	L/R	Width W_{UH}, mm	Thickness t_{UH}, mm	Width of slotted hole w_{sl}, mm
120	288	2.40	50	10	10

distribution of slotted holes, and other geometric properties such as the aspect ratio of the length of flatted part to the radius of curved part. Based on the findings, the dimension of UH dampers applicable to a base isolator was determined as shown in Table 3.

3. Experimental Validation of U-Shaped Hysteretic Damped Base Isolation Systems

3.1. Structural properties of laminated-rubber bearings

In order to confirm structural properties of a laminated-rubber bearing with the same dimensions as shown in Table 2, four cyclic tests were performed with the constant vertical load of 150 kN. Each test was loaded with increasing displacement amplitudes, 100, 150, and 170 mm which are equivalent to about 100, 150, and 170% shear strain of the total height (105 mm) of rubber layers, respectively. Once finishing a cyclic test with the imposing displacement amplitudes, the next cyclic test was carried out again after sufficient time lag that is required to return to the undeformed shape of a laminated-rubber bearing. The deformed shapes of the laminated-rubber bearing observed in the cyclic test are presented in Fig. 5.

From the tests, the lateral stiffness of the laminated-rubber bearing is evaluated for each imposed displacement level and is summarized in Table 4. The lateral stiffness measured during three cycles for each imposed displacement level is almost constant. However, the lateral stiffness is decreased with increasing the imposed displacement levels.

This is the common properties examined at laminated-rubber bearings. The decreased lateral stiffness causes the increased period Tf of an isolator, as shown in Table 4. Although the periods Tf calculated from the measured lateral stiffness Kf are longer compared to the target period of 3.0 second, this change is allowable in that the increased period improves the seismic response of an isolated structure.

3.2. Structural properties of UH dampers

Cyclic tests of UH dampers were performed to investigate their structural properties which influence on the seismic response of a base isolated structure. UH dampers are inevitably deformed in both lateral directions − in-plane and out-of-plane directions of U-shaped steel strip − when they are subjected to ground shaking. The hysteretic behavior of UH dampers has excitation direction-dependency. Suzuki *et al.* (2005) and Kwon (2008) found that UH dampers under in-plane loading have higher yield strength and initial stiffness but lower post-yielding stiffness ratio compared to those under out-of-plane loading.

A set of two U-shaped steel strips made from HTS was used for a cyclic test to consider their excitation direction-dependency. As shown in Fig. 6, one of them was placed in the same direction as loading while the other was placed to induce the out-of-plane deflections. Vertical loads were not applied to the specimen with the assumption that a laminated-rubber bearing carries all of gravity loads. An actuator attached on the rigid sliding plate on
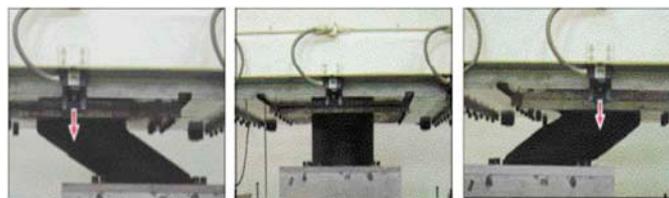
Figure 5. Cyclic test of a laminated-rubber bearing.

Table 4. Lateral stiffness and corresponding period of a base isolator per each imposed displacement level

Tests	lateral stiffness, K_f (N/mm) and corresponding period of an isolator T_f (second)					
	100% shear strain		150% shear strain		170% shear strain	
	K_f	T_f	K_f	T_f	K_f	T_f
Test 1	62		58	3.23	54	3.34
Test 2	62	3.12	58	3.23	56	3.28
Test 3	62		58	3.23	56	3.28
Test 4	62		57	3.25	55	3.31

(a) Loading in left direction   (b) At original position   (c) Loading in right direction

(d) Hysteretic behavior of UH dampers   (e) Bilinear approximation
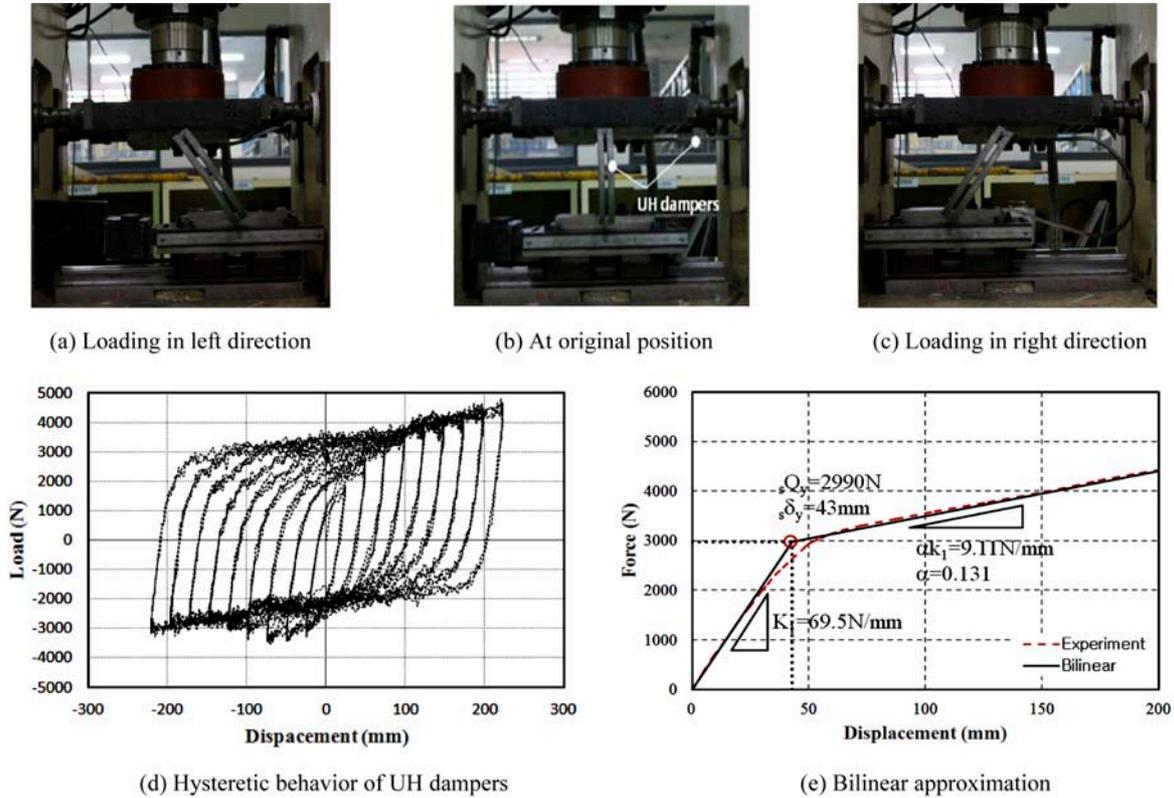
Figure 6. Cyclic tests of UH dampers.

frictionless sliding rails was used as a loading apparatus.

Figure 6 (d) presents the hysteretic curve obtained from the cyclic test. Stable force-displacement relation was observed even at the large displacement level of 200 mm which is larger than the design maximum displacement of 185 mm obtained from (11). For the design of UH dampers, the hysteretic curve is assumed as the bilinear response shown in Fig. 6 (e). The yield strength $Q_{Y,s}$, the corresponding displacement $\delta_{Y,s}$, and the elastic stiffness $k_{I,s}$ of a set of two U-shaped steel strips are, respectively, 3.0 kN, 43 mm, and 69.5 N/mm. The post-yielding stiffness ratio α_s defined as the ratio of the stiffness after yielding to the elastic stiffness is 0.131. Large portion of the post-yielding stiffness ratio is due to the post-yielding behavior of the U-shaped steel strip deformed in the out-of-plane direction. The response of UH dampers to cyclic loading including the improvement of deformation capabilities due to the introduction of slotted holes on a U-shaped steel strip is found in Kwon (2008) in detail.

3.3. Shake-table tests of a fix-based structure, a base-isolated structure without UH damper, and a base-isolated structure with UH dampers

In order to study the seismic response of base-isolated structures with UH dampers experimentally, three frame specimens were prepared; 1) a fix-based two-story steel MRF (FMRF), 2) a base-isolated two-story steel MRF without UH dampers (BMRF), and 3) that with UH

dampers (BMRFD). The two-story steel MRF designed in the previous section was used for all specimens. The specimens were mounted on a shake-table whose the table size is 5 meter by 5 meter and the maximum acceleration, velocity, and stroke under nominal payload of 500 kN are, respectively, 1.25 g, 1,000 mm/sec, and 300 mm. A total 300 kN weigh steel blocks − 150 kN weigh steel blocks per each floor − was mounted on the floors. Figure 7 (a) shows the test set-up of the FMRF specimen with a braced safety frame. In order to measure absolute acceleration and relative displacement of each floor, and strain of each structural member, LVDTs, accelerometers, strain gauges, and Vision System which can measure the movements of pre-defined target points, such as Target 1 to 17 in Fig. 7 (b), were installed.

For the BMRF and BMRFD specimens, a total two laminated-rubber bearings were installed and each laminated-rubber bearing was placed at the middle of each footing girder in the parallel with the direction of shaking. Frictionless sliding bearings were located at the end of the columns to remove unexpected restraints and to increase structural global stability of the isolated frame. Four UH dampers made from HTS were installed at each laminated-rubber bearing. Two of them were placed in the same direction as shaking and the other two were located in the transverse direction to the shaking direction.

The records used for the shake-table tests were obtained from the Elcentro earthquake, as shown as Fig. 2 (a). The

(a) Test set-up   (b) Measurements
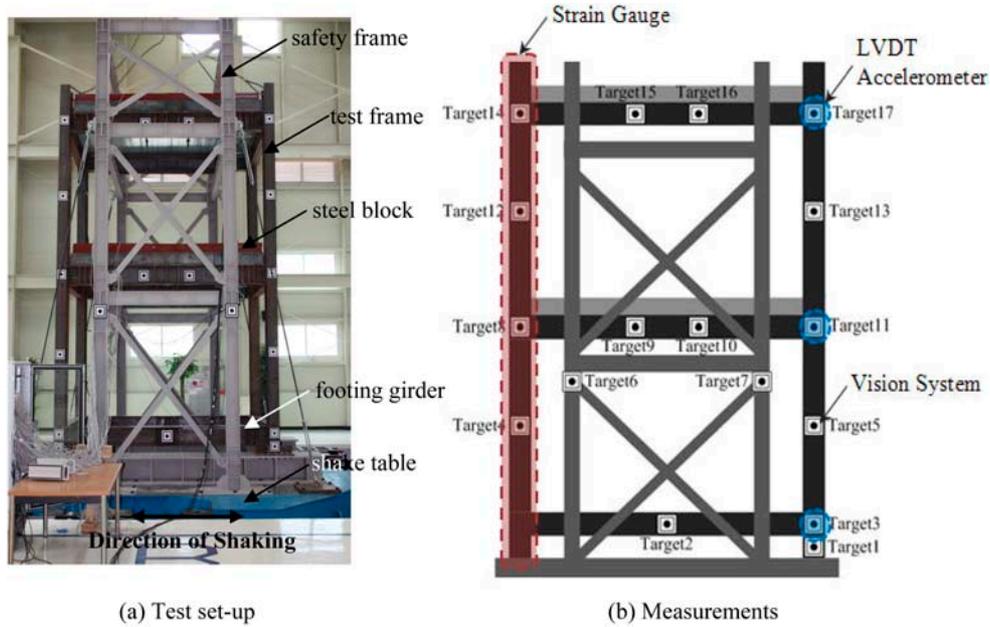
Figure 7. Test set-up and measurements for shake-table tests.

(a) 1ˢᵗ story drift response   (b) 2ⁿᵈ story drift response
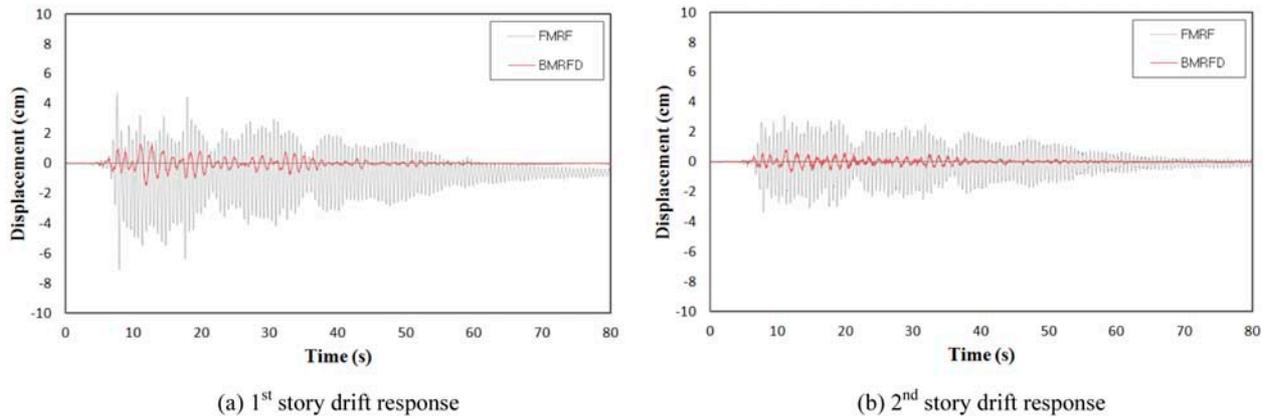
Figure 8. Story drift time-history of FMRF and BMRFD specimens under Elcentro record with 1.0 scale factor.

peak ground acceleration is 0.364 g and the dominant periods are 0.2, 0.5~1.0, and 3 seconds. Since the fundamental period 0.54 and 0.195 second of the fixed base structure considered is similar to the dominant periods of the record, it is possible that the test frame can experience important structural response stages from elastic to plastic behavior although the acceleration capacity of the shake table is relatively low with considering the seismic weight of 300 kN. Except the BMRF specimen, each specimen was shaken with incremental ground accelerations using scale factors of 0.3, 0.4, 0.7, 1.0, 1.3, 1.6, and 2.0. The BMRF specimen was excited up to the ground accelerations with the scale factors of 0.3 and 0.4 to re-use the steel frame for the BMRFD specimen.

Before the FMRF, BMRF and BMRFD tests, free vibration tests of the steel MRF were carried out to measure the fundamental periods and damping ratios calculated by amplitude decay. Also, resonance tests of the steel MRF were performed to investigate an equivalent viscous damping ratios. Test results show that the fundamental period and equivalent viscous damping ratio for the 1ˢᵗ mode of vibration are 0.577 second and 1.39 % of critical, respectively. This fundamental period is a good agreement with the period of 0.54 second obtained from the analysis.

3.3.1. Cyclic response of FMRF, BMRF, and BMRFD tests

3.3.1.1. Story drift time-history response

Figure 8 shows the story drift time-history of the FMRF and BMRFD specimens under the Elcentro record with a scale factor of 1.0. The absolute maximum story drifts of the FMRF specimen were examined to 70.9 mm (equal to 2.8% of story height) and 33.9 mm (equal to 1.36% of story height) for the 1ˢᵗ and 2ⁿᵈ story, respectively. On the other hand, the absolute maximum story drifts of

(a) Using scale factor = 0.3

(b) Using scale factor = 0.4

(c) Using scale factor = 0.7

(d) Using scale factor = 1.0

(e) Using scale factor = 1.6

(f) Using scale factor = 2.0
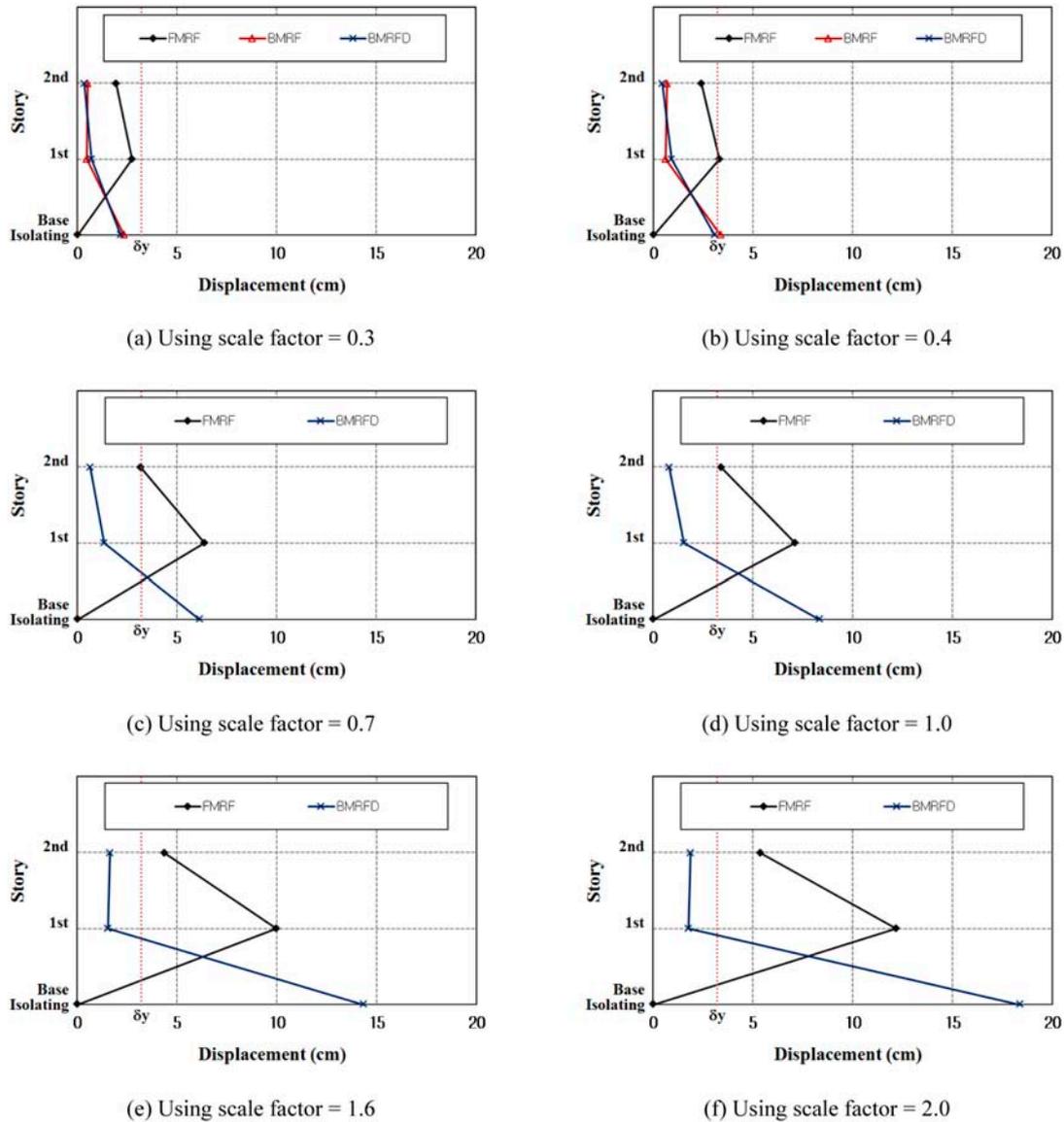
Figure 9. Absolute maximum story drifts of FMRF, BMRF, and BMRFD specimens.

83.4, 15.3, and 8 mm were, respectively, observed in the base isolated floor, 1st and 2nd story. It is also shown from Fig. 8 that the cyclic period of the BMRFD specimen is longer than that of the FMRF specimen because of the period lengthening effect due to the base isolating systems. This result demonstrates that the elongated structural periods due to the introduction of the base isolating systems and the added damping capacity from UH dampers cause significant reduction of the story drift response and the concentration of story drifts on the laterally flexible base isolating floor. After shaking residual drift of 7 mm was remained in the 1st story of the FMRF specimen but any residual drift was not examined in the BMRFD specimen except the base isolating floor where residual drift of 4.1 mm was remained.

Figure 9 summarizes absolute maximum story drifts of the FMRF, BMRF, and BMRFD specimens under the Elcentro ground motions with scale factors of 0.3, 0.4, 0.7, 1.0, 1.6, and 2.0. The difference of the peak story drift response between the FMRF and BMRFD specimens becomes prominent as the intensities of ground acceleration are increasing. While the maximum story drifts of the BMRFD specimen is limited to 18.8 mm (equal to 0.75% of story height), the peak story drifts of the FMRF specimen reaches to 4.9% of story height when both are subjected to a ground motion with scale factor of 2.0. For the ground motions with scale factors of 0.3 and 0.4, the BMRF and BMRFD specimens show similar peak response since UH dampers in the BMRFD specimen are in the elastic range such that supplemental energy dissipation cannot be expected. The FMRF specimen started to experience structural damages when subjected to the ground motion scaled by 0.7. This was demonstrated from the observation of residual drifts of 0.6 and 0.4 mm

(a) Structural damages observed in the FMRF specimen   (b) Deformed shape of a laminated rubber bearing and UH dampers
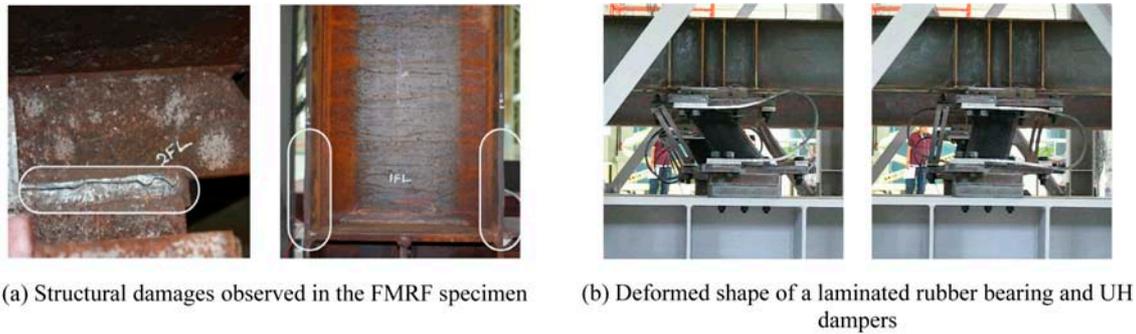
Figure 10. Member response of FMRF, and BMRFD specimens.

at the 1st and 2nd story. Residual drifts of the FMRF specimen were increased with increasing scale factors. Figure 10 presents the structural damages of the FMRF specimen such as cracks at the beam-to-column interface and local buckling in the column flanges, and the deformed shapes of a laminated-rubber bearing and in-plane and out-of-plane UH dampers.

3.3.1.2. Base shear time-history response

Using the measured absolute acceleration time-history at each floor during the shake-table tests, base-shear forces can be calculated and their absolute maximum values are summarized in Table 5. Values in parentheses of the table are the ratios of maximum base-shear forces obtained from the BMRF and BMRFD tests to that of the FMRF test. The ratios ranges from 0.17 for the ground motion scaled by 0.3 to 0.29 for the ground motion scaled by 2.0. This means that frames above base isolating systems can be designed with lower base shear compared to fix-based frames. The base-shear force and roof

displacement relations of the FMRF and BMRFD specimens under the ground motion with scale factors of 1.0 and 1.6 are shown in Fig. 11. The figure also illustrates the bilinear hysteretic behavior of the FMRF specimen and energy dissipation due to the UH dampers in the BMRFD specimen. The stable hysteretic response of the BMRFD specimen demonstrates that the UH dampers installed to induce deformations in both their in-plane and out-of-plane directions sustain even at large displacement levels without any stiffness and strength degradation. It is also shown from the hysteretic curve of the BMRFD test that the use of HTS material and the introduction of the slotted-hole details effectively work on increasing the deformation capacity of UH dampers.

3.3.1.3. Input energy and dissipated energy

Using inherent equivalent viscous damping ratio of the FMRF, accelerations and displacements measured at each story in the FMRF and BMRFD specimens, energy dissipation of each story and total input energy can be

Table 5. Maximum base shear response of FMRF, BMRF, and BMRFD specimens

Specimens	Measured maximum base shear in kN along scale factors of ground motion						
	0.3	0.4	0.7	1.0	1.3	1.6	2.0
FMRF	144.3	172.6	221.0	233.7	232.0	239.0	251.7
BMRF	5.9(0.04)	8.1(0.05)	-	-	-	-	-
BMRFD	24.5(0.17)	29.1(0.17)	40.4(0.18)	43.8(0.19)	49.0(0.21)	54.1(0.23)	72.3(0.29)

(a) Using scale factor = 1.0   (b) Using scale factor = 1.6
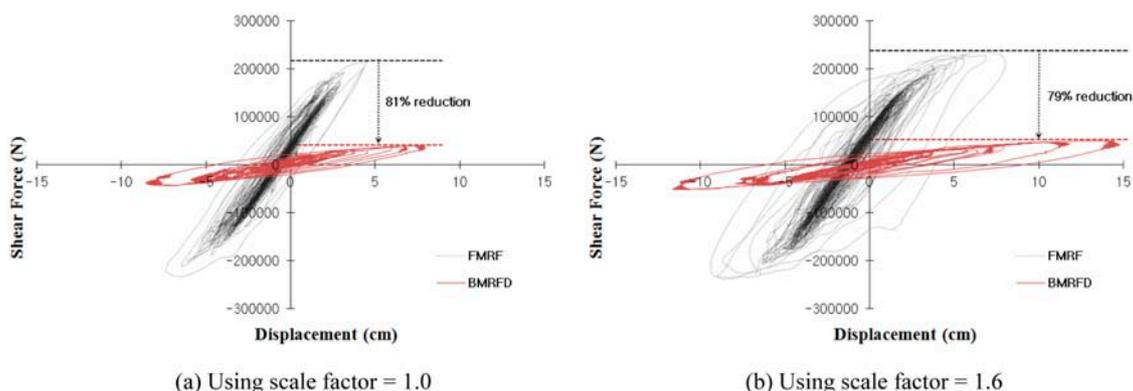
Figure 11. Base shear-roof displacement relation of FMRF and BMRFD specimens.

(a) FMRF specimen
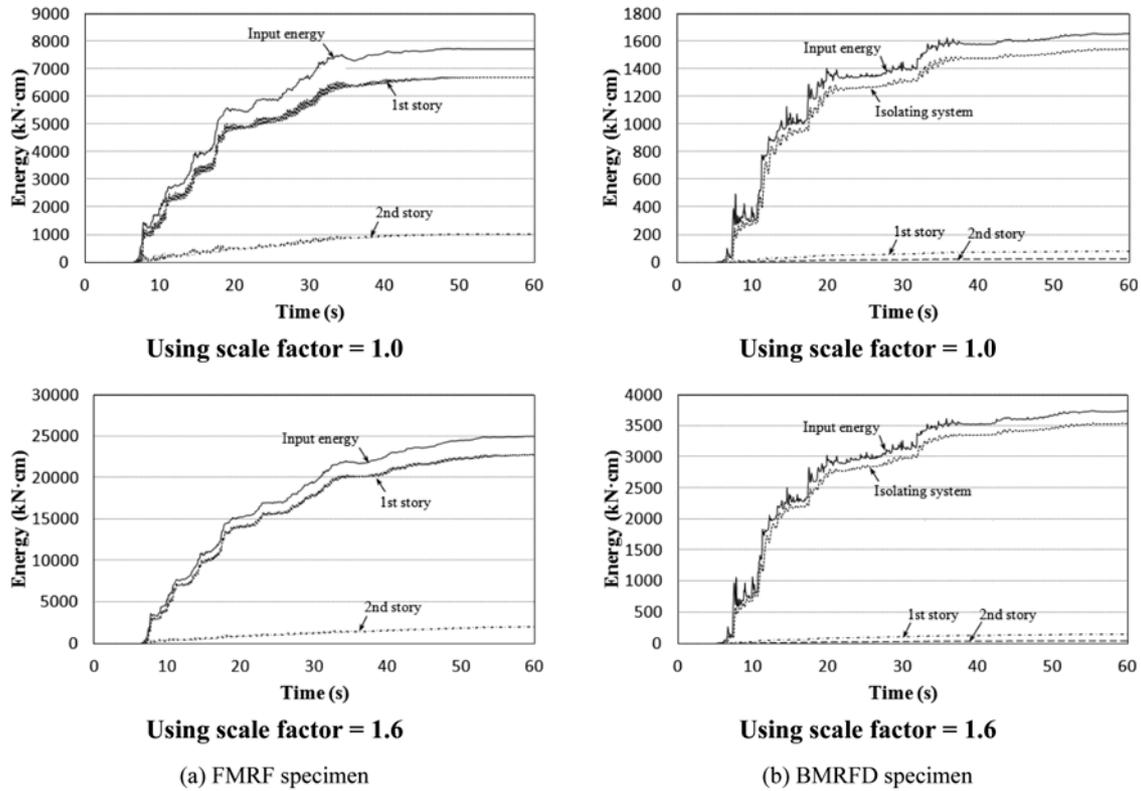
(b) BMRFD specimen

Figure 12. Input energy and energy dissipation of FMRF and BMRFD specimens.

obtained and are presented in Fig. 12 for the ground motions with scale factors of 1.0 and 1.6. Input energy of the FMRF specimen was remarkably larger than that of the BMRFD specimen. Scale factors used for the ground motion increase with increasing input energy and dissipated energy of both specimen, as shown in Table 6 where summarizes the energy response obtained from the FMRF and BMRFD specimens under the ground motion scaled by the factors.

Most of energy dissipation occurred at the 1st story in the FMRF specimen because of the plastic behavior (ultimately structural damages) of the columns in the 1st story. This was more prominent as the scale factor increases. On the other hand, significantly large portion of the input energy measured in the BMRFD specimen

was dissipated or absorbed in the base isolating floor mainly due to the hysteretic behavior of UH dampers. Thanks to energy dissipation of UH dampers, energy dissipation of the steel MRF above the base isolating floor was negligible, which means structural damages are controlled. It is desirable features to protect structures from earthquake attack in that the replacement of UH dampers after severe ground shaking makes them to be functional.

3.3.2. Discussion on energy-based design procedure of base isolating systems

The maximum base shear of 43.8 kN at the BMRFD specimen under the ground motion with scale factor of 1.0 is similar to the assumed design base shear of 46.4

Table 6. Input energy and dissipated energy of FMRF and BMRFD specimens

Specimens			Input energy and dissipated energy in kN·cm						
			0.3	0.4	0.7	1.0	1.3	1.6	2.0
FMRF	Input energy		354	814	3,835	7,716	8,878	24,971	47,626
	Dissipated Energy	1 story	248	572	3,143	6,686	7,766	22,845	44,294
		2 story	106	240	631	1,008	1,086	2,056	3,204
BMRFD	Input energy		171	293	846	1,656	2,648	3,746	5,433
	Dissipated Energy	Isolator	151	260	776	1,546	2,495	3,550	5,175
		1 story	16	25	36	84	114	146	188
		2 story	4	7	11	25	35	46	62

Table 7. Equivalent velocities of FMRF and BMRFD specimens

Specimens	Measured equivalent velocities in cm/sec along scale factors of ground motion						
	0.3	0.4	0.7	1.0	1.3	1.6	2.0
FMRF	49.8	75.8	144.2	197.6	208.7	397.7	577.6
BMRFD	29.4(0.59)	41.3(0.54)	71.9(0.50)	97.1(0.49)	130.8(0.63)	144.8(0.36)	181.1(0.31)

Table 8. Value of h measured at FMRF and BMRFD specimens

Specimens	Measured equivalent velocities in mm/sec along scale factors of ground motion						
	0.3	0.4	0.7	1.0	1.3	1.6	2.0
FMRF	0.41	0.94	5.18	11.02	12.80	37.66	73.01
BMRFD	1.22	2.09	6.24	12.44	20.08	28.56	41.26

kN. The estimation of maximum base shear from the energy-based design procedure is within allowable tolerance. However, the maximum displacement 83.4 mm measured at the base isolating floor in the BMRFD specimen is different with the displacement δ_m=185 mm calculated from Eq. (11) with design values of T_f=3.0 second, V_{EM} =150 cm/sec and η=8.0. The deviation between the measured and calculated maximum displacements is mainly due to the conservative estimation of V_{EM} and η. The deviation of velocity is verified by the comparison the value of V_{EM} with the equivalent velocity V_{exp} calculated from total input energy estimated from the measured accelerations and displacements during a shake-table test. The measured V_{exp} is, as shown in Table 7, 97.1 cm/ second equal to $0.64V_{EM}$ when the BMRFD specimen is subjected to the ground motion with scale factor of 1.0. The use V_{exp} of instead of V_{EM} in estimating maximum displacements leads δ_m=120 mm, which produces more accurate prediction. Table 7 indicates that the intensities of the ground motions increase with the increase of the input energy which is directly related to the equivalent velocity shown in Eq. (7). Especially the equivalent velocity is almost linearly proportional to the scale factors for the ground motion. Values in parentheses of Table 7 are the ratios of equivalent velocities of the BMRFD specimen to those of the FMRF specimen. The ratios are relatively constant ranging 0.49 to 0.63 for the ground motions with scale factors, from 0.3 to 1.3. For the ground motions with scale factors of 1.6 and 2.0, the ratios are decreased to 0.36 and 0.31 since the remarkable expansion of plastic response in the FMRF specimen increases the input energy, which consequently the equivalent velocity of the FMRF increases.

Value of η is important in predicting the maximum displacement in the energy-based design procedure. Following Akiyama's suggestion (1985; 1988), 8 was assigned to η. Table 8 presents η values computed using the displacement response at the base isolation floor and the bilinear approximation shown in Fig. 6 (b). Similar to the observation of energy equivalent velocities, the values of η also significantly increase for the FMRF specimen

under the ground motion with scale factors of 1.6 and 2.0 whereas the values of η steadily increase with the increase of scale factors. With V_{exp}=97.1 cm/second and η=12.44 at scale factor of 1.0, a re-evaluated maximum displacement that base isolators experience is 94.9 mm which becomes relatively good estimation to the measured displacement of 83.4 mm. It is, however, important to mention that such conservative estimation of V_{EM} and η in predicting the maximum displacements occurring at the base isolating floor could be allowable in that uncertainty relating to the duration and intensities of earthquakes and doubtable hysteretic response of base isolated structures should be considered in the design phase.

4. Conclusion

This paper proposes a base isolating system to reduce the seismic demands of a low- or medium- rise structure and experimentally investigates the seismic response of the base isolated structure throughout shake-table tests after designing it according to energy balance seismic design procedure. The base isolating system considered in this study consists of laminated-rubber bearings and U-shaped hysteretic (UH) dampers which are made of high toughness steel (HTS) and are machined with slotted holes to increase their deformation capacity.

A base isolated 2-story steel moment-resisting frame (MRF) and base isolating system consisting of laminated-rubber bearings and UH dampers were first designed for shake-table tests using energy balance design methodology. Cyclic tests of components, a laminated-rubber bearing and UH dampers, for the base isolating systems were then carried out to investigate their structural properties and to confirm that their properties match with the design values. The component tests for the laminated-rubber bearing show excellent deformation capacity with some degree of its deformation-dependency. The measured lateral stiffness kf and corresponding period Tf of the laminated-rubber bearing are in allowable tolerance in design phase. The test results for the UH dampers show the stable hysteretic

response even at significantly large displacement levels. This demonstrates that the introduction of HTS material and slotted holes increases the deformation capacities of the UH dampers by inducing uniform stress distribution along a U-shaped steel strip.

Finally, shake-table tests with FMRF, BMRF, and BMRFD specimens were performed using Elcentro ground motion records scaled by several factors, 0.3, 0.4, 0.7, 1.0, 1.3, 1.6, and 2.0. Noticeable structural damages due to the plastic behavior of 1st story columns were observed at the FMRF specimen under the ground motions with scale factor of 1.0, 1.3, 1.6, and 2.0. On the other hand, shake-table tests of the BMRFD specimen show that the proposed base isolating system with UH dampers limits the seismic demands of a base isolated structure by lengthening the structural periods, concentrating displacement demands on the base isolating floor and adding seismic energy dissipation from the UH dampers. The ratios defining the maximum base-shear forces obtained from the BMRFD tests to those of the FMRF test ranges from 0.17 to 0.29. From this it is found that frames above base isolating systems consisting of laminated-rubber bearings and UH dampers can be designed with lower base shear compared to fix-based frames. Input energy into the FMRF specimen is remarkably larger than that of the BMRFD specimen and most of energy dissipation occurred at the 1st story in the FMRF specimen while significantly large portion of the input energy measured in the BMRFD specimen was dissipated or absorbed in the base isolating floor mainly due to the hysteretic behavior of UH dampers.

The design values calculated from the energy balance design procedure were compared with the corresponding test results. The maximum base shear of the BMRFD specimen is in good agreement with the design base shear. However, the maximum displacement measured at the base isolating floor in the BMRFD specimen was different with the displacement calculated during the energy balance design procedure. This deviation is mainly due to the conservative estimation of V_{EM} and η. The re-evaluation of the maximum displacement at a base isolating floor with V_{EM} and η measured at the shake table tests leads the improved estimation.

Acknowledgments

References

Akiyama, H. (1985). *Earthquake-Resistant Limit-State Design for Buildings.* University of Tokyo Press, Tokyo, Japan (in Japanese).

Akiyama, H. (1988). "Earthquake resistant design based on the energy concept." *Proc. 9th World Conference on Earthquake Engineering*, Tokyo-Kyoto, Japan, pp. 905-910.

ASCE (2000). Prestandard and Commentary for the Seismic Rehabilitation of Buildings. *FEMA-356*, American Society of Civil Engineers, Reston, Virginia, USA.

BSSC (1997). NEHRP Guidelines for the Seismic Rehabilitation of Buildings. *FEMA-273*, Building Seismic Safety Council, Washington D.C., USA.

BSSC (2003). NEHRP Recommended Provisions for the Seismic Regulations for New Buildings and Other Structures: Parts 1 and 2. *FEMA-450*, Building Seismic Safety Council, Washington D.C., USA.

Christopoulos, C. and Filiatrault, A. (2006). *Principles of Passive Supplemental Damping and Seismic Isolation*, IUSS Press, Pavia, Italy.

Cousins, W. J., Robinson, W. H., and McVerry, G. H. (1991). "Recent developments in devices for seismic isolation." *Proc. Pacific Conference on Earthquake Engineering*, Christchurch, New Zealand, pp. 221-232.

Housner, G. W. (1956). "Limit design of structures to resist earthquakes." Proc. 1st WCEE, California, USA, pp. 1-11.

Housner, G. W. (1959). "Behavior of structures during earthquakes." *Proc. of the American Society of Civil Engineering*, EM4, pp. 109-129.

Hwang, J. S. and Ku, S. W. (1997). "Analytical modeling of high damping rubber Bearings." *Journal of Structural Engineering*, 123(8), pp. 1029-1036.

Kelly, J. M. (1979). "Aseismic base isolation: A review." *Proc. 2nd National Conference on Earthquake Engineering*, California, USA, pp. 823-837.

Kelly, J. M. (1990). "Base isolation: Linear theory and design." *Earthquake Spectra*, 6(2), pp. 223-244.

Kwon, S. I. (2008). Structural performance evaluation of steel damper for seismic isolation system with material property and shape. *Master's Thesis*, Pusan National University, Korea (in Korean).

MIDAS Gen (2008). *MIDAS Gen* (Ver. 741) – *User's manual.* Midas IT, Seoul, Korea (in Korean).

Pan, P., Zamfiresku, D., Nakashima, M., Nakayaso, N., and Kashiwa, N. (2004). "Base-isolation design practice in Japan: Introduction to the Post-Kobe approach." *Journal of Earthquake engineering*, 9(1), pp. 1-25.

Parducci, A. and Mezzi, M. (1991). "Seismic isolation of bridges in Italy." *Proc. Pacific Conference on Earthquake Engineering*, Christchurch, New Zealand, pp. 45-56.

Robinson, W. H. (1982). "Lead-rubber hysteretic bearings suitable for protecting structures during earthquake." *Earthquake Engineering and Structural Dynamics*, 10(4), pp. 593-604.

SEAOC (1995). *Vision 2000 – Performance-Based Seismic Engineering of Buildings.* Structural Engineering Association of California, Sacramento, CA, USA.

Skinner, R. I., Robinson, W. H., and McVerry, G. H. (1993). *An Introduction to Seismic Isolation*, John Wiley & Sons, New York, USA.

Soong, T. T. and Dargush, G. F. (1997). *Passive Dissipation Systems in Structural Engineering*, John Wiley & Sons, New York, USA.

Suzuki, K., Watanabe, A., and Saeki, E. (2005). "Development of U-shaped steel damper for seismic isolation system." *Nippon Steel Technical Report No. 92*, Japan (in Japanese).

Teramura, A., Takeda, T., Tsunoda, T., Seki, M., Kageyama, M., and Nohata, A. (1988). "Study on earthquake response characteristics of base-isolated full scale building." *Proc. 9th World Conference on Earthquake Engineering*, Tokyo-Kyoto, Japan, pp. 693-698.

Tyler, R. G. (1977). "Design of steel plate devices for seismic energy dissipation, European seismic design practice: Research and Applications." *Proc. 5th SECED Conference*, Chester, UK, pp. 445-453.